Khalkhali *et al.*, ***BioImpacts,*** 2015, 5(3), 141-150
doi: 10.15171/bi.2015.19
http://bi.tbzmed.ac.ir/

Synthesis and characterization of dextran coated magnetite nanoparticles for diagnostics and therapy

Maryam Khalkhali[1], Somayeh Sadighian[2], Kobra Rostamizadeh[3,4*], Farhad Khoeini[1], Mehran Naghibi[5], Nahid Bayat[2], Mina Habibizadeh[2], Mehrdad Hamidi[3]

[1] Department of Physics, University of Zanjan, Zanjan, Iran
[2] Department of Pharmaceutical Biomaterials, School of Pharmacy, Zanjan University of Medical Sciences, Zanjan, Iran
[3] Zanjan Pharmaceutical Nanotechnology Research Center, Zanjan University of Medical Sciences, Zanjan, Iran
[4] Department of Medicinal Chemistry, School of Pharmacy, Zanjan University of Medical Sciences, Zanjan, Iran
[5] Shahid Beheshti University of Medical Sciences, Tehran, Iran

Article Info

Article Type:
Original Article

Article History:
Received: 06 June 2015
Revised: 16 June 2015
Accepted: 22 June 2015
ePublished: 30 June 2015

Keywords:
Magnetic nanoparticles
Curcumin
Dextran
MRI contrast agent

Abstract

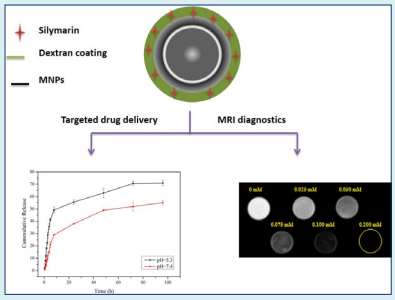

Introduction: Expansion of efficacious theranostic systems is of pivotal significance for medicine and human healthcare. Magnetic nanoparticles (MNPs) are known as drug delivery system and magnetic resonance imaging (MRI) contrast agent. MNPs as drug carriers have attracted significant attention because of the delivery of drugs loaded onto MNPs to solid tumors, maintaining them in the target site by an external electromagnetic field, and subsequently releasing drugs in a controlled manner. On the other hand, it is believed that MNPs possess high potential as MRI contrast agents. The aim of this work was to payload curcumin into dextran coated MNPs and investigate their potential as theranostic systems for controlled drug delivery and MRI imaging.

Methods: MNPs were synthesized as a core and coated with dextran as polymeric shell to provide steric stabilization. Curcumin as anticancer drug was selected to be loaded into NPs. To characterize the synthesized NPs, various techniques (e.g., DLS, FESEM, FT-IR, XRD, and VSM) were utilized. In vitro drug release of curcumin was evaluated at 37˚C at the pH value of 5.4 and 7.4.The feasibility of employment of dextran coated MNPs as MRI contrast agents were also studied.

Results: Formulations prepared from dextran coated MNPs showed high loading (13%) and encapsulation efficiency (95%). In vitro release study performed in the phosphate-buffered saline (PBS, pH= 7.4, 5.4) revealed that the dextran coated MNPs possess sustained release behavior at least for 4 days with the high extent of drug release in acidic media. Vibrating sample magnetometer (VSM) analysis proved the superparamagnetic properties of the dextran coated MNPs with relatively high-magnetization value indicating that they were sufficiently sensitive to external magnetic fields as magnetic drug carriers. Furthermore, dextran coated MNPs exhibited high potential as T_2 contrast agents for MRI.

Conclusion: Based on our findings, we propose the dextran coated MNPs as promising nanosystem for the delivery of various drugs such as curcumin and MRI contrast agent.

Introduction

Nanoparticles (NPs) composed of organic building blocks have widely been studied for the delivery drugs and genes. For example, liposomes, polymersomes, dendrimers,[1-3] polymeric NPs and micelles[4,5] are in various steps of preclinical and clinical development.[6] Inorganic NPs have obtained intensive attention in recent years due to their specific physicochemical properties which are not sometimes feasible in organic NPs. Particularly unique optical properties, stability, magnetic properties, possibility of functionalization, and other physical properties make inorganic NPs attractive systems for imaging and drug delivery purposes in comparison to organic nanoparticles. Amongst, superparamagnetic iron oxide nanoparticles (SPIONs) are especially interesting because of their unique magnetic properties, biocompatibility, and good

***Corresponding author:** Kobra Rostamizadeh, Email: Rostamizadeh@zums.ac.ir

© 2015 The Author(s). This work is published by BioImpacts as an open access article distributed under the terms of the Creative Commons Attribution License (http://creativecommons.org/licenses/by-nc/4.0/). Non-commercial uses of the work are permitted, provided the original work is properly cited.

bioadaptability.[7,8] MNPs have been employed in many technologies such as hyperthermia treatments, drug delivery,[9] MRI contrast agents, magnetic separation,[10] and recyclable catalysts.[11]

However, in order to have the benefit of both organic and inorganic materials, nanocomposites have recently been introduced.[12,13] For instance, in order to improve the MNPs characteristics for drug delivery goals such as colloidal stability, it has been shown that their coatings with hydrophilic organic polymers[14] such as dextran can be considered as a valuable strategy. The synthesis of magnetite/polymer NPs can generally be achieved through three methods; (a) assembling MNPs and polymer nanoparticles after being prepared separately via physicochemical or physical interactions between two compounds,[15] (b) in situ precipitation of MNPs in the presence of polymer, and (c) in situ polymerization of monomers in the presence of MNPs. MNPs have been widely studied as T_2 contrast agents in MRI because of enhancement of the negative contrast (darkness) in phantom images by T_2 relaxivity of water protons.

Dextran as a naturally made polysaccharide possesses poly-cationic and hydrophilic properties and could be found in certain lactic acid bacteria, *Leuconostoc mesenteroides* and *Streptococcus mutans*, holding α-d (1-6) and α-d (1-3) linked glucose branch units.[16,17]

Curcumin, a natural polyphenolic phytoconstituent, is derived from *Curcuma longa* Linn (Zingiberaceae) and has various pharmacological properties.[18] The bis-α, β-unsaturated β-diketone is the chemical structure of curcumin (Fig. 1).[19] Curcumin is a well-known natural anti-inflammatory agent owing to the inhibitory properties of cyclooxygenase-2 (COX-2), lipoxygenase, and persuadable nitric oxide synthase (iNOS) enzymes.[20-24] In addition, it displays high potential for the medicinal therapy of different illnesses, particularly cancer.[25,26] However to attain the maximum efficacy of curcumin, low solubility is a major challenge. To avoid the low solubility and consequently low bioaccessibility of curcumin, nanoscaled drug delivery approaches have been proposed, [27] including liposomes,[28] solid lipid nanoparticles (SLNs),[29] chitosan-based NPs,[30] or NPs complexed with phospholipids,[31] and cyclodextrin.[32]

In the present study, the aim was to investigate the applicability of MNPs for both drug delivery and non-invasive MRI monitoring. Dextran coated MNPs were prepared and loaded with curcumin with the purpose of simultaneous controlled drug delivery and MRI imaging.

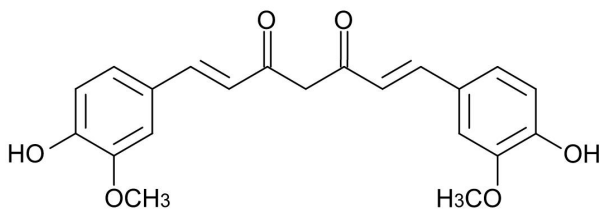

Fig. 1. Chemical structure of curcumin.

Materials and methods

Chemical materials

Ferric chloride hexahydrate ($FeCl_3 \cdot 6H_2O$), ferrous chloride tetrahydrate ($FeCl_2 \cdot 4H_2O$), NH_4OH (25% of ammonia), dextran (13-20 kDa), 1,1-diphenyl-2-picryl hydrazyl radical (DPPH), Dimethyl sulfoxide (DMSO), and curcumin were purchased from Merck (Darmstadt, Germany). Dialysis tubing (molecular weight cut-off 12,000), 3-[4, 5 dimethylthiazol-2-yl]-2, 5-diphenyltetrazolium bromide (MTT), and trypan blue was purchased from Sigma-Aldrich (St. Louis, MO, USA). MDA-MB-231 cell line was bought from Pasteur Institute of Iran. Dulbecco's Modified Eagle Medium (DMEM) cell culture medium, fetal bovine serum (FBS), and penicillin/streptomycin were obtained from ATOCEL (Budapest, , Hungary). 96-well cell culture plates and flasks were from SPL Life Science Co. (Pocheon-si, Gyeonggi-do, South Korea). All materials were used as received, without any purification.

Preparation of dextran coated MNPs

The MNPs were synthesized by co-precipitation method. Briefly, first N_2 gas was bubbled into 45 mL distilled water. Then, 1mmol of $FeCl_2 \cdot 4H_2O$, 2mmol of $FeCl_3 \cdot 6H_2O$, and 5 mL of 0.5% dextran were added to the solution, then NH_4OH was added drop-wise by syringe. After stirring of mixture at 60°C under N_2 for 30 min, a black suspension was formed. The black precipitate was separated by centrifuge at 1500 rpm for 15 min. The product was dried at room temperature.

Preparation of curcumin-loaded dextran coated MNPs

Briefly, dextran coated MNPs (50 mg) was added into 10 mg curcumin (preliminarily solubilized in 5 mL ethanol) and stirred for 20 h. The curcumin loaded dextran MNPs were separated by centrifugation at 14000 rpm and then washed (3×) with deionized water. The curcumin entrapped nanoparticles were dried in vacuum oven at 30°C for 12 h. The unloaded curcumin was determined by measuring the concentration of drug in the supernatant by UV-Vis spectrophotometry at wavelength of 425 nm. The entrapment efficiency was calculated using the equation (1):

$$\text{Entrapment Efficiency}(\%) = \frac{(\text{Total amount of drug} - \text{free amount of drug})}{\text{total amount of drug}} \times 100 \quad (1)$$

Drug release study

The release of drug molecules from NPs were studied in phosphate-buffered saline (PBS) containing 0.5% (w/v) Tween™ 80 in physiological pH of 7.4 and acidic media with the pH value of 5.3. Typically, 10 mg of NPs were placed into a dialysis bag (cut off 12 kDa) and introduced to 15 mL of PBS with desired pH under stirring at 100 rpm at 37°C. At predetermined time intervals, in order to determine the drug concentration in dialysate and thereby time dependent drug release profile, 1.0 mL of dialysate

was taken out and replaced with 1.0 mL of fresh buffer solution maintained at 37°C and assayed by UV–Vis spectroscopy at wavelength of 425 nm.

Characterization methods

Fourier transformed infrared (FT-IR) spectroscopy was recorded with Mattson 1000 FT-IR spectrometer using KBr pellets in the region of 400–4000 cm^{-1}. The morphology of the dextran coated MNPs was studied by field-emission scanning electron microscopy (FESEM, Mira 3-XMU). The magnetic properties of MNPs and the dextran coated MNPs were measured in vibrating sample magnetometer (VSM, Lake Shore 7400) with an applied field between 20 to 20 kOe at 25°C. The particle size distribution of the prepared core-shell was determined by dynamic light scattering (DLS) (Malvern Instruments, UK, model Nano ZS). The structure and crystal phase of the dextran coated MNPs were measured by a Bruker D8 X-ray diffractometer with monochromated high-intensity Cu Ka radiation (k =1.5418 Å) operated at 40 kV and 30 mA.

Magnetic resonance imaging (MRI)

The feasibility of employment of dextran coated MNPs as MRI contrast agents was studied by plotting T_1 relaxation rate ($1/T_1$) and T_2 relaxation rate ($1/T_2$) as a function of Fe concentration which their slope subsequently results in calculation of the longitudinal relaxivity (r_1) and transverse relaxivity (r_2), respectively. To achieve this goal, T_1 and T_2 weighted phantom MRI images of dextran coated MNPs with different Fe concentrations of 0, 25, 50, 75, 100, and 200 µM were obtained at a field strength of 1.5 T at 25°C by using a clinical whole body magnetic resonance (MR) scanner (Siemens Healthcare Avanto, Germany). In order to obtain both T_1 and T_2 relaxation times, a number of spin-echo sequences were run.

The T_1 relaxation times were estimated at various repetition times of 100, 1550, 3150, 4750, and 6400 ms with an echo time of 18 ms, slice thickness: 7.5 mm, field of view (FOV): 230, and matrix: 200×256. The T_2 relaxation values were determined with repetition time (TR) of 1600 ms and varying echo times (TE) of 10, 43, 79, 108, and 140 ms, slice thickness: 7.5 mm, field of view (FOV): 238, Turbo factor: 18, and matrix: 176×384.

After taking the images, signal intensity was measured within manually-drawn regions of interest (ROI) for each sample with the help of Dicom Works 1.3.5 software. Relaxation rates R_1 ($1/T_1$) and R_2 ($1/T_2$) were calculated by mono-exponential curve fitting of the signal intensity vs. time (TE or TR) based on the equations (2) and (3):[33,34]

$$I = M_0[1-\exp\left(-\frac{TR}{T_1}\right) \quad (2)$$

$$I = M_0 \exp\left(-\frac{TE}{T_2}\right) \quad (3)$$

where, I is the signal intensity and M_0 is constant.

In vitro radical scavenging activity of curcumin loaded MNPs

In order to measure free radical scavenging activity, decolorization property of the stable DPPH was used in the presence of antioxidants, that is, curcumin and curcumin loaded dextran coated MNPs. DPPH radical scavenging activity of nanoparticle was determined as follows: Briefly, the different concentrations of curcumin were prepared in methanol (0.006-0.06 mM). Curcumin solution was protected from light. Equal volumes of each of the concentrations of curcumin (1 mL) were added to the test containers containing DPPH (100 mM) and following the incubation for 30 min, absorbance was read at 517 nm. Triplicate experiments were performed for each sample. Scavenging activity was calculated using the formula (4):

$$DPPH\ radical\ scavenging\ activity(\%) = \frac{A_C - A_S}{A_C} \times 100 \quad (4)$$

Where, A_C is the absorbance of the control, and A_S is the absorbance of extract or standard sample. Finally, IC_{50} value was calculated which was defined as the concentration of the sample required to decrease the absorbance at 517 nm by 50%.

Cytotoxicity assay

Curcumin was dissolved in DMSO. Dextran coated MNPs and curcumin loaded MNPs were used in aqueous form. Human breast adenocarcinoma cell line, MDA-MB-231, was cultured in DMEM culture medium supplemented with 10% FBS and penicillin/Streptomycin at 37°C in a humidified atmosphere with 5% CO_2. The cells were then seeded in 96-well cell culture plate at the density of 10^4 cells/well, 24 h prior to treatment with increasing concentrations 1, 5, 10, 50, and 100 µg/mL of studied materials including curcumin, curcumin loaded MNPs, and dextran coated MNPs. Desired drug concentrations were prepared in complete cell culture medium and DMSO concentration was not more than 1% v/v in any of treatments. Cell viability was assessed after 24 h and 48 h using MTT colorimetric survival assay. Briefly, 20 µL of MTT solution (5 mg/mL in PBS) was added to each well and the plate was incubated in humidified CO_2 incubator for 4 h. Mitochondrial enzymes, NADPH-oxidoreductases, can reduce the tetrazolium salt MTT to formazan crystals which are soluble in DMSO. Therefore, formazan formation indicates the presence of living cells. The medium were then removed and formazan crystals were dissolved in 100 µL DMSO. The absorption was quantified using plate reader at wavelengths of 570 nm. The reference wavelength was 690 nm. Cell viability (%) was calculated as the ratio of the number of surviving cells in drug-treated samples to that of control. The data were analyzed using GraphPad Prism software (version 5.0). One-way analysis of variance (ANOVA) was performed and group means were compared by Tukey post-hoc test. Values were considered statistically significant at P value ≤ 0.05.

Results

Physicochemical characterization of curcumin loaded MNPs

The FT-IR spectra were recorded to prove the successful preparation of curcumin loaded MNPs and possible interaction between various constituents of nanoparticles. FT-IR spectrum of the MNPs (a), dextran coated MNPs (b), free curcumin (c), and curcumin loaded dextran coated MNPs are shown in Fig. 2. FT-IR spectrum of MNPs (spectrum a) exhibits the band at 578 cm^{-1} which is assignable to the absorption of ν (Fe–O), and the broad absorption peak appeared at about 3429 cm^{-1} can be related to the presence of hydroxyl groups. Comparing spectra a and b, some new absorption bands are appeared. For instance, the bands at about 1028, 1015, and 1155 cm^{-1} were due to the stretching vibration of the alcoholic hydroxyl (C–O), and the band at 1404 cm^{-1} was attributed to the bending vibration of C–H bond. These data proved that the surface of MNPs has been covered with dextran polymer.[35,36] It is believed that different interactions such as van der Waals force, hydrogen bond, and electrostatic interactions keep dextran on the surface of MNPs.

As shown in Fig. 2 (spectrum c), the FT-IR results exhibit the broad absorption band at 3423 cm^{-1} indicating the presence of phenolic O–H group. Furthermore, an absorption band at 1629 cm^{-1} attributed to stretching vibrations of benzene ring, absorption peak at 1508 cm^{-1} imputed to C=O, band at 1430 cm^{-1} indicates functional group of olefinic C–H bending vibration and 1280 cm^{-1} can be assigned to the aromatic C–O stretching vibration.[37] By comparing spectra c and d, the characteristic peaks of curcumin in curcumin loaded MNPs are distinguishable even though the main region of spectra are overlapped. In other words, it clearly demonstrated that curcumin was successfully entrapped in dextran coated MNPs.

The X-ray diffraction patterns of MNPs and dextran coated MNPs samples are shown in Fig. 3. A series of characteristic peaks for MNPs at 2θ (111, 220, 311, 400, 422, 511, and 440) were observed for MNPs (spectrum a), and dextran coated MNPs (spectrum b) which are characteristic peaks of MNPs. The intensities of MNPs diffraction peaks for dextran coated MNPs were weaker than those of the naked MNPs, which indicate the presence of dextran on the surface of MNPs. The average particle size calculated using Debye Scherer's formula for naked and dextran coated MNPs, were 10.48 and 12.83 nm, respectively.

Fig. 4 shows the magnetization curves of the naked MNPs and dextran coated MNPs. The results showed that both samples exhibited superparamagnetic properties. The saturation magnetization values (M_s) of the MNPs and dextran coated MNPs were 80.152 and 70.572 emu/g, respectively. As shown in Fig. 4, the saturation magnetization was reduced following the coating of MNPs with dextran. The finding can be explained by the presence of dextran on the surface of MNPs. It was shown that the thickness of shell was determinant parameter in the extent of magnetization decrease; whatever the density of shell increased, the magnetism decreased.

The size of MNPs before and after surface modification was

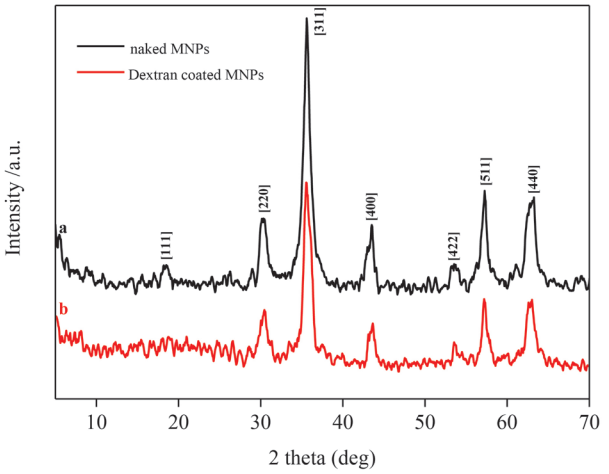

Fig. 3. XRD pattern of (a) the naked MNPs and (b) dextran coated MNPs

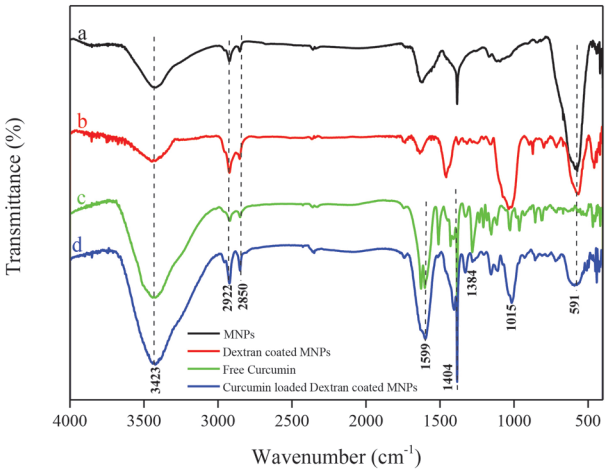

Fig. 2. FT-IR spectra of MNPs (a), dextran coated MNPs (b), free curcumin (c), and curcumin loaded dextran coated MNPs (d).

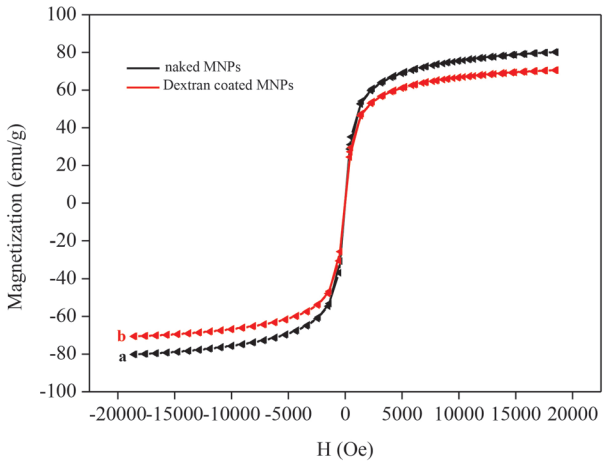

Fig. 4. Magnetization vs. applied magnetic field of (a) uncoated and (b) dextran coated MNPs

investigated by DLS analysis. In the case of naked MNPs, the size of nanoparticles was about 126 nm (Fig. 5A). The particle size distribution curves exhibited only one peak with a relative high polydispersity index indicating the MNPs aggregation in solution. The size of dextran coated MNPs was also analyzed by DLS. The results showed that the particle size of dextran coated MNPs decreased to 58 nm (Fig. 5B). Decrease in particle size after dextran coating can be related to the impact of dextran coating on protecting MNPs from aggregation which consequently results in high dispersion capability of MNPs.

Morphology of the MNPs was studied by FESEM technique. Fig. 5 (panels C and D) represents the quasi-spherical morphology of MNPs and dextran coated MNPs with the average size of 55 and 17 nm, respectively.

Zeta potential measurement evaluates the surface charge of nanoparticles and can be indicative of the extent of their stability. For MNPs and dextran coated MNPs, the zeta potential value was obtained to be −24.2 and −16.9 mV, respectively. Apparently, coating MNPs with dextran caused a significant decrease in zeta potential (Figs. 5E and F). It is believed that the negative value of zeta potential for MNPs arises from the existence of OH^- groups on the surface of MNPs. Thereby, reduction in surface charge after dextran coating can be evidence of hydrogen bonding between the O^- groups of dextran and hydroxyl group of MNPs.

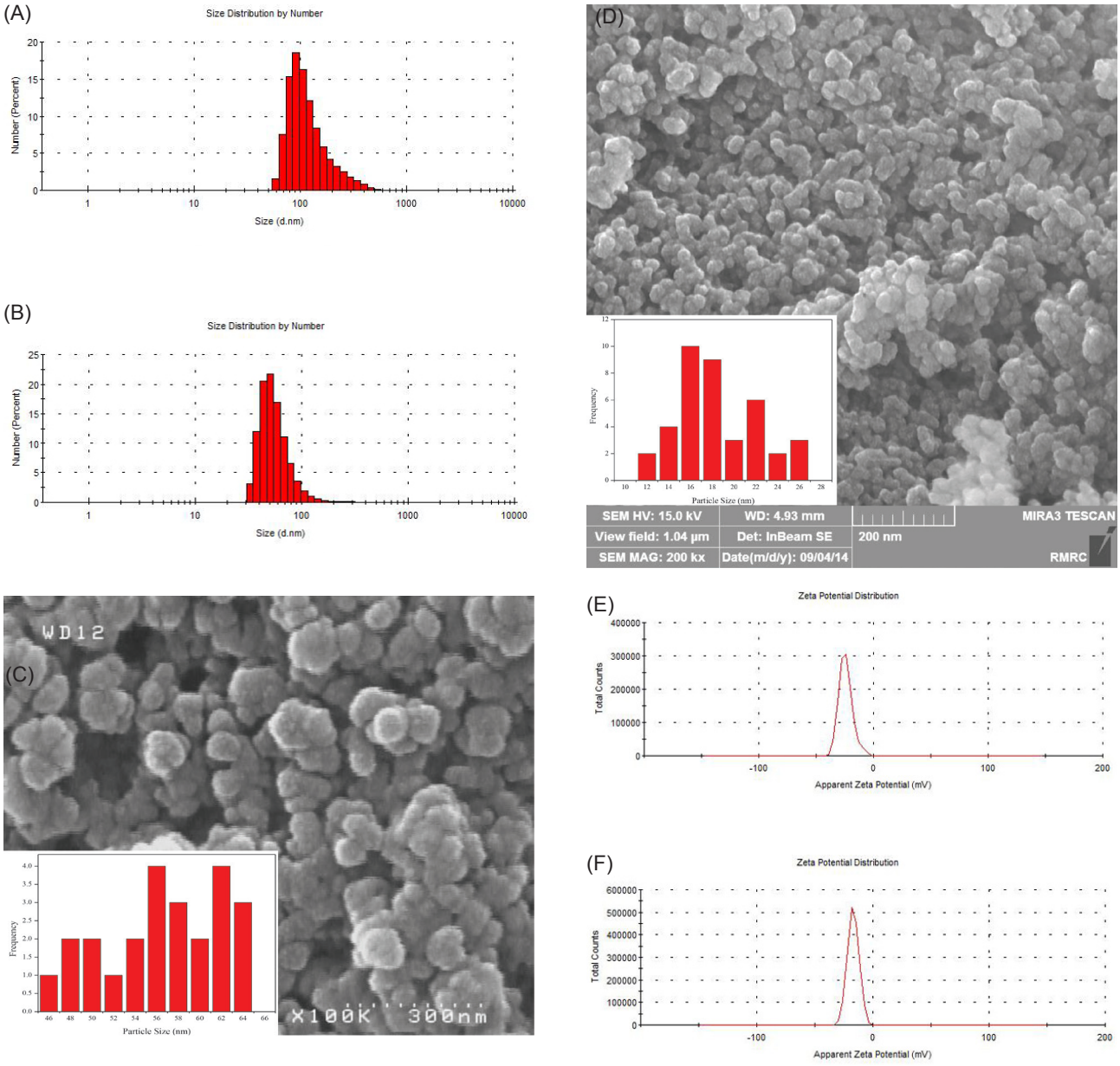

Fig. 5. Size, morphology and zeta potential of MNPs. A) DLS particle size distribution of MNPs. B) DLS particle size distribution of dextran coated MNPs. C) Electron microscopy micro-graphs of MNPs. D) Electron microscopy micro-graphs of dextran coated MNPs. E) Zeta potential of MNPs. E) Zeta potential of dextran coated MNPs.

In vitro drug release treatment

The cumulative release of curcumin loaded MNPs was studied in buffer solutions with two different pH values of 5.3 and 7.4 at the physiological temperature of 37°C. The cumulative drug release was expressed as the percent of drug liberation as a function of time. Fig. 6 shows the cumulative release of curcumin from dextran coated MNPs. Of particular note was that drug release at both pHs showed comparatively sustained release behavior. However, as shown in Fig. 6, there was high amount of burst drug release in acidic pH compared to the one at neutral media probably to the high solubility of curcumin in acidic solution. The maximum drug release attainable at neutral and acidic media after 72 h was up to 70% and 40%, respectively (Fig. 6).

Drug release kinetic

To comprehend the mechanisms that control the drug release from dextran coated MNPs, the release data were fitted with some widely used mathematical models including Zero-order, First-order, Gompertz, Korsmeyer-Peppas, Higuchi, Hixson-Crowell, Peppas-Sahlin, and Weibull.[38] The model with the highest determination coefficient (R^2 adjusted) and the minimum Akaike information criterion (AIC) was chosen as the best fit. Data analysis was carried out using the Excel add-in DDSolver program. The findings revealed that in both release condition (neutral and acidic media) release data were adequately fitted to the Peppas-Sahlin model. According to the Peppas-Sahlin model, the values of R^2 for curcumin loaded MNPs in the media with the pH value of 5.3 and 7.4 were found to be 0.9815 and 0.9769, respectively (Table 1). Based upon the structure of engineered NPs, it is believed that the release rate of drug is mainly controlled by the rate of drug diffusion.

MRI contrast enhancement

The proton relaxivity measurements was performed to study the possibility of dextran coated MNPs as MRI contrast agent. The effect of NPs on the longitudinal (T_1) and transverse (T_2) proton relaxation was evaluated using a clinical 1.5 T whole body magnetic resonance (MR) scanner. Fig. 7 shows T_2-weighted MR images of dextran coated MNPs with different Fe concentrations. It is shown that the T_2-weighted images' brightness decreases significantly with the increase of Fe concentration. The observation reveals that dextran coated MNPs can be considered as a good MR T_2 contrast agent under the T_2-imaging sequences. Longitudinal relaxivity (r_1) values were calculated by the linear fit of the equation (5):

$$R_i = \frac{1}{T_i} = \left(\frac{1}{T_i}\right)_0 + r_i C \qquad (5)$$

where, R_i is the relaxation rate, T_{i0} is the relaxation time in the pure water, C is the concentration of the contrast agent, and r_i is relaxivity.

As shown in Fig. 8, there is a linear relationship between the T_1 relaxation rate ($1/T_1$) and Fe concentration. Based on the slope of the line, longitudinal relaxivity was found to be 12.79 $mM^{-1}s^{-1}$ for the dextran coated MNPs.[39] On the other hand, r_2 value was calculated from the slope of linear plots of $1/T_2$ versus Fe concentration as given in Fig. 9. Dextran coated MNPs demonstrated transversal relaxivity value of 220.20 $mM^{-1}s^{-1}$. The calculated r_1, r_2, and r_2/r_1 values are shown in Table 2. The relaxivity ratio, r_2/r_1, was calculated to be 17.21 which is higher than that of Resovist, commercially available MRI contrast agent[40] indicating that dextran coated MNPs are feasible to be used as negative MRI contrast agents. In other words, dextran coated MNPs can be used as T_2 MRI contrast agents and consequently they are able to decrease the MR signal intensity by dephasing of proton spins.

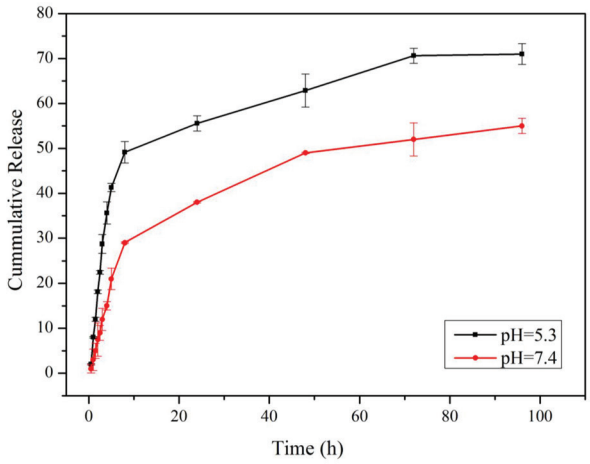

Fig. 6. In vitro drug release profile of curcumin from dextran coated MNPs at pH= 5.3 and 7.4.

In vitro radical scavenging activity of curcumin loaded MNPs

Determination of scavenging activity with the DPPH stable radical is a common method to evaluate the free radical scavenging ability of various compounds. DPPH is a free radical that is stable at room temperature and produces a purple color when dissolved in ethanol. This solution becomes colourless in the presence of an antioxidant. It should be stated that this method is fast, reliable and easy. In the present study, the scavenging activity of curcumin and curcumin loaded MNPs were determined by DPPH assay. The results on the DPPH scavenging ability from curcumin and curcumin-loaded dextran-coated MNPs are shown in Fig. 10. These results showed that curcumin and curcumin-loaded dextran-coated MNPs have similar power of antioxidant activities.

Investigation on the radical scavenging activity showed that curcumin and curcumin-loaded dextran-coated MNPs had similar power of antioxidant activities with an IC_{50} value of about 6 μM.

Cell viability assay

Results from survival MTT experiments in MDA-MB-231

Table 1. Summary of model parameters for curcumin release kinetics.

Models	Equation[a]	Parameters			
		pH=7.4		pH=5.3	
Zero-order	$F = K_0 t$	R^2	0.8868	R^2	0.5350
		AIC	-25.1350	AIC	-12.9668
		MSE	0.0061	MSE	0.0249
		k0	0.108	k0	0.038
Gompertz	$F = 100 \times exp\{-\alpha \times exp[-\beta \times \log t]\}$	R^2	0.9642	R^2	0.8961
		AIC	-33.4850	AIC	-25.9496
		MSE	0.0022	MSE	0.0063
		α	6.523	α	6.746
		β	0.327	β	0.240
Korsmeyer-Peppas	$F = kkp \times t^n$	R^2	0.9478	R^2	0.8723
		AIC	-30.1041	AIC	-23.8941
		MSE	0.0032	MSE	0.0077
		kKP	0.160	kKP	0.131
		n	0.764	n	0.563
Higuchi	$F = K_H \sqrt{t}$	R^2	0.8478	R^2	0.8607
		AIC	-22.4738	AIC	-25.0234
		MSE	0.0082	MSE	0.0074
		kH	0.232	kH	0.151
Hixson-Crowell	$1 - \sqrt[3]{1-F} = k_{\frac{1}{3}} t$	R^2	0.8877	R^2	0.5367
		AIC	-25.2091	AIC	-13.0038
		MSE	0.0061	MSE	0.0248
		kHC	0.000	kHC	0.000
Peppas-Sahlin	$F = k_1 t^m + k_2 t^{2m}$	R^2	0.9815	R^2	0.9769
		AIC	-37.4165	AIC	-38.9911
		MSE	0.0013	MSE	0.0016
		k1	-1.151	k1	0.074
		k2	1.275	k2	-0.002
		m	0.142	m	1.104
Weibull	$F = 100 \times \left[1 - exp\left[-\frac{(t-T_i)^\beta}{\alpha}\right]\right]$	R^2	0.9792	R^2	0.9046
		AIC	-36.3805	AIC	-24.8035
		MSE	0.0015	MSE	0.0066
		α	378.020	α	624.015
		β	0.534	β	0.501
		Ti	0.844	Ti	0.496
First-order	$F = 100 \times [1 - exp(-k_1 \times t)]$	R^2	0.8882	R^2	0.5376
		AIC	-25.2462	AIC	-13.0224
		MSE	0.0061	MSE	0.0247
		k1	0.001	k1	0.000

[a]F indicates fraction of drug released up to time t. k0, α, β, kKP, n, kH, kHC, k1, k2, m, α, β, Ti, and k1 are parameters of the models.

cells are presented in Fig. 11. The free curcumin showed a significant cytotoxic effect in a time and dose dependent manner. Furthermore, the results indicated that dextran coated MNPs and curcumin loaded MNPs did not have any significant cytotoxicity in a 24 or 48 h treatment period on MDA-MB-231 cells.

Discussion

MNPs were prepared using the co–precipitation of ferric and ferrous salts in alkaline medium based upon the reactions (6) and (7):

$$NH_4OH \leftrightarrow NH_4^+ + OH^- \quad (6)$$

$$Fe^{2+} + 2Fe^{3+} + 8OH^- \leftrightarrow Fe_3O_4 + 4H_2O \quad (7)$$

It is believed that MNPs synthesized by this method tend to aggregate. To reduce the aggregation of nanoparticles and enhance the therapeutic efficacy of curcumin, while increasing the solubility, dextran shell was introduced on the surface of MNPs. The carrier was composed of MNPs in order to direct carrier towards tumor sites by the employment of an external magnetic field. It can simultaneously be used as MRI contrast agent. Curcumin was entrapped via hydrogen bonding and electrostatic interactions with the ability to release the entrapped drug in the low pH environment (pH 5.0–5.5) simulating the acidic environment of the endosomes. It should be expressed that the low pH environment (pH 5.0–5.5) of the endosome of the cancer cells is widely used for the endosmal escape of anticancer drugs in the targeted therapy of solid tumors by nanomedicines. The release behavior of engineered nanocarrier was examined in buffer solutions with different pHs (i.e., 5.3 and 7.4). The highest liberation of drug molecules was found to be in acidic solution medium (i.e., over 70% at pH 5.3

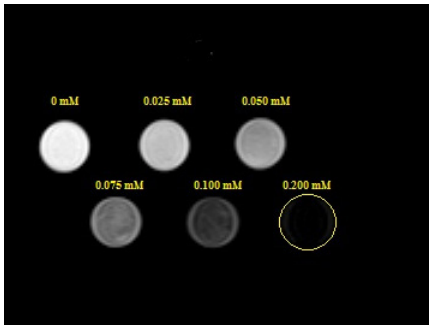

Fig 7. T_2-weighted MRI images (1.5T, spin-echo sequence: repetition time TR = 1600 ms, echo time TE = 79 ms) of the dextran coated MNPs at various iron concentrations at 25°C.

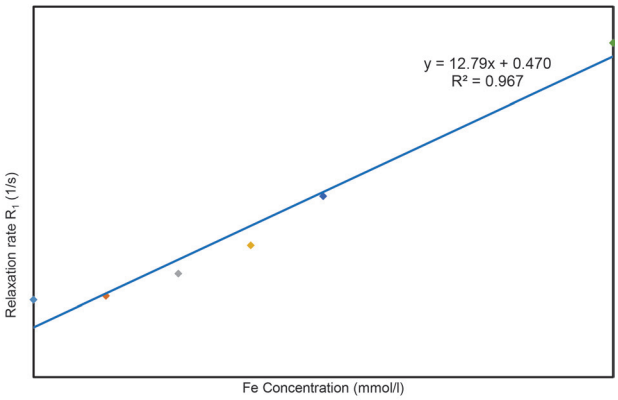

Fig 8. T_1 relaxation rate plotted as a function of Fe concentration (mM) for dextran coated MNPs.

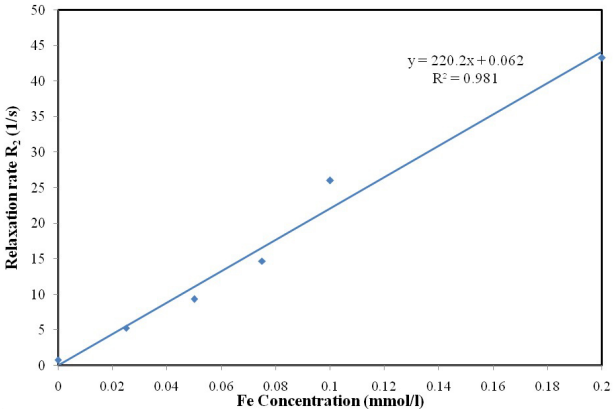

Fig 9. T_2 relaxation rate plotted as a function of Fe concentration (mM) for dextran coated MNPs.

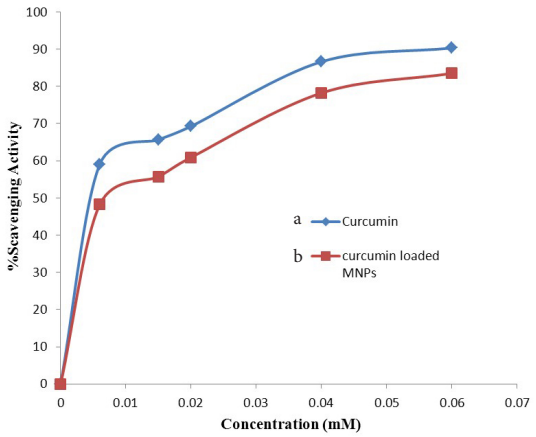

Fig 10. Scavenging Activity of curcumin (a) and curcumin loaded MNPs (b).

in comparison with 50% at pH 7.4 after 4 days). On the other hand, dextran loaded MNPs showed a considerable potential as T_2 MR contrast agent with the relaxivity ratio value of 17.21. The IC_{50} of both curcumin itself and curcumin loaded MNPs were found to be similar. This indicates that curcumin loaded MNPs display similar radical scavenging activity in comparison with the free curcumin (Fig. 10), while the drug liberation profile showed controlled release behavior.

In the cytotoxicity assay in human breast cancer MDA-MB-231 cells (Fig. 11), free curcumin showed a significantly higher cytotoxicity than those of the synthesized MNPs and curcumin loaded MNPs. It was expected to face somewhat higher toxic impacts by the curcumin loaded MNPs after 48 h post-treatment. However, we speculate that the liberation of curcumin molecules from the MNPs is largely time-dependent and hence the cytotoxicity studies need to be considered for a longer time period.

Conclusions

Magnetic nanoparticles were successfully synthesized by co-precipitation method. In order to avoid the agglomeration of MNPs, dextran was used as polymeric shell on MNPs. The anticancer curcumin molecules were loaded onto the dextran coated MNPs. Curcumin MNPs were characterized using various techniques including FT-IR, FESEM, and DLS. The size of MNPs was decreased after surface coating, while it did not impose any effect on the morphology of NPs. Study of magnetic property of prepared MNPs proved their superparamagnetic nature. Dextran loaded MNPs showed considerable potential as

Table 2. Magnetic resonance imaging properties. The longitudinal relaxivity (r_1, $mM^{-1}s^{-1}$), transverse relaxivity (r_2, $mM^{-1}s^{-1}$), r_2/r_1 values and R^2 of dextran coated magnetite nanoparticles was calculated by plotting the T_1 relaxation rate ($1/T_1$) and T_2 relaxation rate ($1/T_2$) as a function of Fe concentration

Nanoparticles	r_1 ($mM^{-1}s^{-1}$)	R^2	r_2 ($mM^{-1}s^{-1}$)	R^2	r_2/r_1
Dextran coated MNPs	12.79	0.967	220.20	0.981	17.21

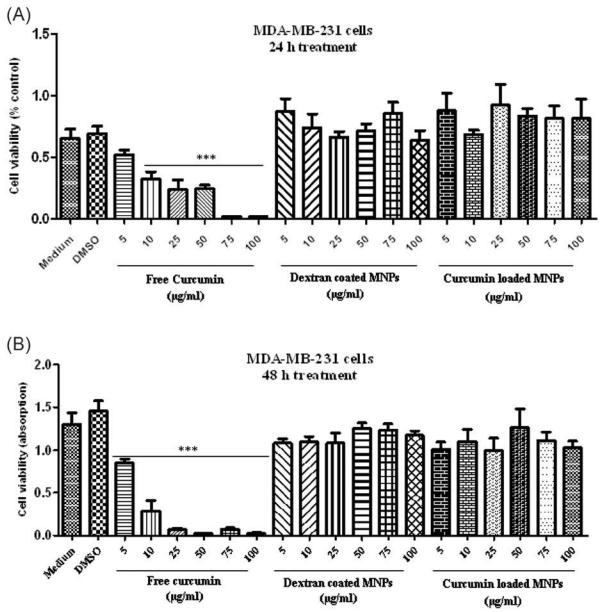

Fig. 11. Cell viability assay. MDA-MB-231 cells were treated with free curcumin, dextran coated MNPs and curcumin loaded MNPs. Cell viability was determined by MTT assay after 24h (A) and 48 h (B).

T_2 MR contrast agent with the relaxivity ratio value of 17.21 (Table 2). The IC_{50} of both curcumin and curcumin loaded MNPs via DPPH method was found to be about 6 μM indicating considerable potential of curcumin loaded MNPs as targeted drug delivery and diagnostic agent for cancer therapy. Based upon the cytotoxicity assay, it can be concluded that these surface modified MNPs can be considered as a safe and biocompatible nanocarriers for the drug delivery and diagnostics purposes.

Research Highlights

What is current knowledge?

√ MNPs possess high potential as MRI contrast agents.

√ Surface modified MNPs can be served as targeted drug delivery systems.

√ Drug loaded MNPs could provide opportunity to design a theranostic system for simultaneous responsive drug delivery and MRI imaging.

What is new here?

√ Curcumin was successfully loaded onto dextran coated MNPs.

√ The carrier showed pH sensitive and controlled drug release characteristics.

√ The potential of curcumin loaded MNPs as MRI T2 contrast agent was proved.

√ Curcumin loaded MNPs showed a high free radical scavenging activity with IC_{50} of 6 μM.

Acknowledgments

Authors are grateful to Zanjan University of Medical Sciences and the University of Zanjan for the financial support. Authors also like to acknowledge the cooperation of Tabesh Medical Imaging Center (Dr. M. H. Abdkarimi) Tabriz, Iran, for acquiring the MRI images.

Ethical issues

No ethical issues to be declared.

Competing interests

The authors declare no conflict of interests.

References

1. Hartner WC, Verma DD, Levchenko TS, Bernstein EA, Torchilin VP. ATP-loaded liposomes for treatment of myocardial ischemia. *Wiley Interdisciplinary Reviews: Nanomedicine and Nanobiotechnology* **2009**; 1: 530-9. doi: 10.1002/wnan.46
2. Bangham A, Standish MM, Watkins J. Diffusion of univalent ions across the lamellae of swollen phospholipids. *Journal of Molecular Biology* **1965**; 13: 238-IN27. doi:10.1016/S0022-2836(65)80093-6
3. Namazi H, Adeli M. Dendrimers of citric acid and poly (ethylene glycol) as the new drug-delivery agents. *Biomaterials* **2005**; 26: 1175-83. doi: 10.1016/j.biomaterials.2004.04.014
4. Gref R, Minamitake Y, Peracchia M, Trubetskoy V, Torchilin V, Langer R. Biodegradable long-circulating polymeric nanospheres. *Science* **1994**; 263: 1600–3. doi: 10.1126/science.8128245
5. Oba M, Vachutinsky Y, Miyata K, Kano MR, Ikeda S, Nishiyama N, et al. Antiangiogenic gene therapy of solid tumor by systemic injection of polyplex micelles loading plasmid DNA encoding soluble Flt-1. *Molecular Pharmaceutics* **2010**; 7: 501-9. doi: 10.1021/mp9002317
6. Service R. Nanotechnology. Nanoparticle Trojan horses gallop from the lab into the clinic. *Science* **2010**; 330: 314. doi: 10.1126/science.330.6002.314
7. Akl MA, Atta AM, Yousef AE-FM, Alaa MI. Characterization of stabilized porous magnetite core–shell nanogel composites based on crosslinked acrylamide/sodium acrylate copolymers. *Polymer International* **2013**; 62: 1667-77. doi: 10.1002/pi.4464
8. Huang H-C, Barua S, Sharma G, Dey SK, Rege K. Inorganic nanoparticles for cancer imaging and therapy. *Journal of Controlled Release* **2011**; 155: 344-57. doi:10.1016/j.jconrel.2011.06.004
9. Sadighian S, Rostamizadeh K, Hosseini-Monfared H, Hamidi M. Doxorubicin-conjugated core–shell magnetite nanoparticles as dual-targeting carriers for anticancer drug delivery. *Colloids and Surfaces B: Biointerfaces* **2014**; 117: 406-13. doi:10.1016/j.colsurfb.2014.03.001
10. Chen D-X, Sanchez A, Taboada E, Roig A, Sun N, Gu H-C. Size determination of superparamagnetic nanoparticles from magnetization curve. *Journal of Applied Physics* **2009**; 105: 083924. doi: 10.1063/1.3117512
11. Lee KS, Anisur RM, Kim KW, Kim WS, Park T-J, Kang EJ, *et al.* Seed size-dependent formation of Fe_3O_4/MnO hybrid nanocrystals: selective, magnetically recyclable catalyst systems. *Chemistry of Materials* **2012**; 24: 682-7. doi: 10.1021/cm2027724
12. Thompson RB, Ginzburg VV, Matsen MW, Balazs AC. Predicting the mesophases of copolymer-nanoparticle

composites. *Science* **2001**; 292: 2469-72. doi: 10.1126/science.1060585
13. Balazs AC, Emrick T, Russell TP. Nanoparticle polymer composites: where two small worlds meet. *Science* **2006**; 314: 1107-10. doi: 10.1126/science.1130557
14. Sadighian S, Hosseini-Monfared H, Rostamizadeh K, Hamidi M. pH-Triggered Magnetic-Chitosan Nanogels (MCNs) For Doxorubicin Delivery: Physically vs. Chemically Cross Linking Approach. *Adv Pharm Bull* **2015**. doi: 10.5681/apb.2015.016
15. Xulu PM, Filipcsei G, Zrinyi M. Preparation and responsive properties of magnetically soft poly (N-isopropylacrylamide) gels. *Macromolecules* **2000**; 33: 1716-9. doi:10.1021/ma990967r
16. Saraswathy A, Nazeer SS, Nimi N, Arumugam S, Shenoy SJ, Jayasree RS. Synthesis and characterization of dextran stabilized superparamagnetic iron oxide nanoparticles for in vivo MR imaging of liver fibrosis. *Carbohydrate Polymers* **2014**; 101: 760-8. doi: 10.1016/j.carbpol.2013.10.015
17. Xia Z, Wang G, Tao K, Li J. Preparation of magnetite–dextran microspheres by ultrasonication. *Journal of Magnetism and Magnetic Materials* **2005**; 293: 182-6. doi:10.1016/j.jmmm.2005.01.059
18. Anand P, Thomas SG, Kunnumakkara AB, Sundaram C, Harikumar KB, Sung B, et al. Biological activities of curcumin and its analogues (Congeners) made by man and Mother Nature. *Biochemical Pharmacology* **2008**; 76: 1590-611. doi: 10.1016/j.bcp.2008.08.008
19. Epstein J, Sanderson IR, MacDonald TT. Curcumin as a therapeutic agent: the evidence from in vitro, animal and human studies. *British Journal of Nutrition* **2010**; 103: 1545-57. doi:10.1017/S0007114509993667
20. Basnet P, Skalko-Basnet N. Curcumin: an anti-inflammatory molecule from a curry spice on the path to cancer treatment. *Molecules* **2011**; 16: 4567-98. doi:10.3390/molecules16064567
21. Jurenka JS. Anti-inflammatory properties of curcumin, a major constituent of Curcuma longa: a review of preclinical and clinical research. *Altern Med Rev* **2009**; 14: 277.
22. Kohli K, Ali J, Ansari M, Raheman Z. Curcumin: a natural antiinflammatory agent. *Indian Journal of Pharmacology* **2005**; 37: 141. doi: 10.4103/0253-7613.16209
23. Sharma R, Gescher A, Steward W. Curcumin: the story so far. *European Journal of Cancer* **2005**; 41: 1955-68.
24. Anand P, Kunnumakkara AB, Newman RA, Aggarwal BB. Bioavailability of curcumin: problems and promises. *Molecular Pharmaceutics* **2007**; 4: 807-18. **doi:** 10.1021/mp700113r
25. Sun A, Shoji M, Lu YJ, Liotta DC, Snyder JP. Synthesis of EF24-tripeptide chloromethyl ketone: a novel curcumin-related anticancer drug delivery system. *Journal of Medicinal Chemistry* **2006**; 49: 3153-8. **doi:** 10.1021/jm051141k
26. Aggarwal BB, Shishodia S, Takada Y, Banerjee S, Newman RA, Bueso-Ramos CE, et al. Curcumin suppresses the paclitaxel-induced nuclear factor-κB pathway in breast cancer cells and inhibits lung metastasis of human breast cancer in nude mice. *Clinical Cancer Research* **2005**; 11: 7490-8. doi: 10.1158/1078-0432.CCR-05-1192
27. Anand P, Nair HB, Sung B, Kunnumakkara AB, Yadav VR, Tekmal RR, et al. Design of curcumin-loaded PLGA nanoparticles formulation with enhanced cellular uptake, and increased bioactivity in vitro and superior bioavailability in vivo. *Biochemical Pharmacology* **2010**; 79: 330-8. doi: 10.1016/j.bcp.2009.09.003
28. Wang D, Veena MS, Stevenson K, Tang C, Ho B, Suh JD, et al. Liposome-encapsulated curcumin suppresses growth of head and neck squamous cell carcinoma in vitro and in xenografts through the inhibition of nuclear factor κB by an AKT-independent pathway. *Clinical Cancer Research* **2008**; 14: 6228-36. doi: 10.1158/1078-0432.CCR-07-5177
29. Gupta V, Aseh A, Ríos CN, Aggarwal BB, Mathur AB. Fabrication and characterization of silk fibroin-derived curcumin nanoparticles for cancer therapy. *International Journal of Nanomedicine* **2009**; 4: 115. doi: 10.2147/IJN.S5581
30. Das RK, Kasoju N, Bora U. Encapsulation of curcumin in alginate-chitosan-pluronic composite nanoparticles for delivery to cancer cells. *Nanomedicine: Nanotechnology, Biology and Medicine* **2010**; 6: 153-60. doi:10.1016/j.nano.2009.05.009
31. Maiti K, Mukherjee K, Gantait A, Saha BP, Mukherjee PK. Curcumin–phospholipid complex: preparation, therapeutic evaluation and pharmacokinetic study in rats. *International Journal of Pharmaceutics* **2007**; 330: 155-63. doi:10.1016/j.ijpharm.2006.09.025
32. Yallapu MM, Jaggi M, Chauhan SC. Poly (β-cyclodextrin)/Curcumin Self-Assembly: A Novel Approach to Improve Curcumin Delivery and its Therapeutic Efficacy in Prostate Cancer Cells. *Macromolecular Bioscience* **2010**; 10: 1141-51. doi: 10.1002/mabi.201000084
33. Arsalani N, Fattahi H, Nazarpoor M. Synthesis and characterization of PVP-functionalized superparamagnetic Fe_3O_4 nanoparticles as an MRI contrast agent. *Express Polym Lett* **2010**; 4: 329-38. doi: 10.3144/expresspolymlett.2010.42
34. Lee N, Hyeon T. Designed synthesis of uniformly sized iron oxide nanoparticles for efficient magnetic resonance imaging contrast agents. *Chemical Society Reviews* **2012**; 41: 2575-89. **doi:** 10.1039/C1CS15248C
35. Banerjee SS, Chen D-H. Fast removal of copper ions by gum arabic modified magnetic nano-adsorbent. *Journal of Hazardous Materials* **2007**; 147: 792-9. doi:10.1016/j.jhazmat.2007.01.079
36. Hong R, Feng B, Chen L, Liu G, Li H, Zheng Y, et al. Synthesis, characterization and MRI application of dextran-coated Fe 3 O 4 magnetic nanoparticles. *Biochemical Engineering Journal* **2008**; 42: 290-300. doi:10.1016/j.bej.2008.07.009
37. Yallapu MM, Jaggi M, Chauhan SC. β-Cyclodextrin-curcumin self-assembly enhances curcumin delivery in prostate cancer cells. *Colloids and Surfaces B: Biointerfaces* **2010**; 79: 113-25. doi:10.1016/j.colsurfb.2010.03.039
38. Barzegar-Jalali M, Adibkia K, Valizadeh H, Shadbad MRS, Nokhodchi A, Omidi Y, et al. Kinetic analysis of drug release from nanoparticles. *Journal of Pharmacy and Pharmaceutical Sciences* **2008**; 11: 167-77.
39. Illés E, Szekeres M, Kupcsik E, Tóth IY, Farkas K, Jedlovszky-Hajdú A, et al. PEGylation of surfacted magnetite core–shell nanoparticles for biomedical application. *Colloids and Surfaces A: Physicochemical and Engineering Aspects* **2014**; 460: 429-40. doi:10.1016/j.colsurfa.2014.01.043
40. Ma X, Gong A, Chen B, Zheng J, Chen T, Shen Z, et al. Exploring a new SPION-based MRI contrast agent with excellent water-dispersibility, high specificity to cancer cells and strong MR imaging efficacy. *Colloids and Surfaces B: Biointerfaces* **2015**; 126: 44-9. doi: 10.1016/j.colsurfb.2014.11.045